JOURNAL OF APPLIED POLYMER SCIENCE VOL. 14, PP. 2999–3019 (1970)

A Study of Fiber Extrusion in Wet Spinning. II. Effects of Spinning Conditions on Fiber Formation

CHANG DAE HAN and LEON SEGAL, *Department of Chemical Engineering, Polytechnic Institute of Brooklyn, Brooklyn, New York 11201*

Synopsis

A study is carried out to investigate the effects of spinning conditions on fiber formation in the wet-spinning process. The spinning conditions studied are free velocity (and hence free diameter), throughput rate, maximum take-up velocity, jet stretch (the ratio of take-up velocity to free velocity), and filament tension. The coagulating bath temperature and concentration are varied, and three spinnerette diameters are used. The spinning dope is an aqueous solution of polyacrylonitrile in sodium thiocyanate. The present study shows that the coagulating bath concentration influences the spinning tension and maximum take-up velocity. Two thread breakage mechanisms are postulated which take into account the rate of coagulation, spinning tension, and thread velocity. An attempt is made to predict the concentration profile of solvent in the moving filament by simultaneously solving the mass and force balance equations, in which the increase in elongational viscosity along the spinning way is assumed to be mainly due to the hardening process.

INTRODUCTION

In the spinning of commercial fibers, "spinnability" is of prime concern. Qualitatively, this term may be defined as the ability or ease of fiber formation under "normal" spinning conditions. Interrelated with spinnability is the mechanism of "fiber breakage." Fiber breakage is more explicitly defined than spinnability, but the factors influencing fiber breakage are not well understood.[1–3] The continuous production of fibers is dependent upon the "critical" fiber breakage that occurs at or near the face of the spinnerette. This critical breakage is affected by the properties of the spinning solution and by the coagulating bath conditions in wet spinning. The thread breakage which may occur far from the spinnerette face is in all probability caused by mechanical imperfections in the spinning equipment.

In commercial wet spinning, a series of complex simultaneous operations are performed on and within each spun filament. These are: extrusion in the spinnerette hole (with associated shear stress generation and relaxation), fiber elongation, molecular orientation, coagulation, and crystallization. In addition, there occur counterdiffusion of solvent and nonsolvent between the solidified skin and fluid core[3,4] and counterdiffusion between the filament perimeter (coagulated skin) and coagulating bath.[3,5] Ignoring crystallization and heat transfer, a thorough investigation of this system

would involve equations expressing mass transfer, the motion of threads being stretched, and the rheological behavior of the liquid thread in the elongational flow field. Furthermore, the physical constants needed to solve such a system of equations are very difficult to determine under such complex conditions. It is not surprising, therefore, that previous investigations have not dealt thoroughly with these aspects of the spinning process.

Recent work on the wet-spinning process itself has centered on the presentation of process parameters such as free diameter, jet stretch, or flow rate as functions of temperature, spinnerette hole size, etc.[3,6,7] However, many of the more important correlations are not touched upon, probably owing to proprietary restrictions. Han[8] has recently attempted to correlate the rheological properties of spin dope with spinnability in the wet-spinning process.

In part I of this series,[9] the authors presented the experimentally obtained results of the effect of rate of elongation on elongational viscosity. In the present paper, we present the results of an experimental investigation on the effects of spinning conditions on fiber formation in the wet-spinning process. An attempt is also made in the present study to predict the concentration profile of solvent in the filament by solving the mass balance and force balance equations, in which the increase in elongational viscosity along the spinning way is assumed to be mainly due to the hardening process.

THEORETICAL

It is a well-established fact that a free jet of viscoelastic fluid swells upon issuing from a spinnerette, giving rise to a maximum jet swell very near the spinnerette face. When the extruded jet is drawn by the take-up device, the jet deforms under the tension and its diameter decreases with distance along the spinning way. The rate of change of diameter of the jet decreases as a hard "skin" is formed on the surface of the filament. In the following theoretical development we shall consider the deformation of a liquid jet under tension, accompanied by a mass transfer between the moving liquid jet and the coagulating bath.

In wet spinning, the tensile force exerted by the take-up device is balanced primarily by two types of force. The first type, which we define as the rheological force F_{rheo}, is the force required to deform the liquid thread along its length. The second type, which we define as the coagulating force F_{coag}, is the force required to overcome the frictional force exerted by the coagulating medium on the moving thread and the surface tension force. It should be noted that F_{rheo} may be assumed constant along the spinning way, but F_{coag} increases with displacement along the spinning way. In part I of the series,[9] the authors have described how the magnitude of F_{rheo} can be determined from the measurement of the tensile force at the take-up device.

When a liquid thread is deformed in an elongational flow field, F_{rheo} is related to the tensile stress p_{xx} by

$$\frac{F_{\text{rheo}}}{A(x)} = p_{xx} = \eta_E \frac{dV(x)}{dx} \tag{1}$$

where η_E is the elongational viscosity, $dV(x)/dx$ is the rate of elongation, and $A(x)$ is the filament cross-sectional area. $A(x)$ is related to the axial velocity $V(x)$ by

$$A(x) = Q/V(x) \tag{2}$$

where Q is the volumetric flow rate and the filament density is assumed constant.

As was discussed in part I of this series,[9] the elongational viscosity η_E is a function only of rate of elongation in the absence of the hardening process (i.e., coagulation). However, in the presence of hardening, the elongational viscosity depends not only on the rate of elongation, but also on the concentration of solvent in the elongating filament at constant temperature. The dependence of elongational viscosity on solvent concentration has not been studied hitherto, and therefore the authors have assumed the following empirical relation:

$$\eta_E(dV/dx,C) = f(dV/dx)g(C). \tag{3}$$

That is, the effects of solvent concentration and rate of elongation on elongational viscosity can be separated. Elongational viscosity as a function of rate of elongation has been experimentally investigated and reported in part I of this paper.[9] The study indicates that elongational viscosity increases slightly with rate of elongation and then decreases slightly as the rate of elongation approaches the maximum (near the breaking point of the filament). Furthermore, the study indicates that the influence of coagulation on the change of elongational viscosity is predominantly large compared to that of rate of elongation. Therefore, for all practical purposes, elongational viscosity may be assumed independent of rate of elongation, giving rise to the expression

$$\eta_E(C) = 3\eta_0 g(C) \tag{4}$$

where $3\eta_0$ is the well-known Trouton viscosity.[10]

Since the experimental data show that η_E increases with distance x in the elongating filament, $g(C)$ must be a function which relates the decreasing concentration of solvent in the filament to this increasing elongational viscosity. Physically, this concentration decrease is the cause of hardening (coagulation). The following expression for $g(C)$ is assumed based solely on the experimental results[9]:

$$g(C) = 1 + A[C_0 - C(x)] + B[C_0 - C(x)]^2 \tag{5}$$

where C_0 is the initial concentration of solvent in the dope on a polymer-free basis, $C(x)$ is the concentration of solvent in the elongating filament, and

constants A and B are empirical constants to be determined. Thus, use of eqs. (2)–(5) in eq. (1) gives

$$V(x)\frac{dV(x)}{dx} = \frac{F_{\text{rheo}}/Q}{3\eta_0\{1 + A[C_0 - C(x)] + B[C_0 - C(x)]^2\}} \tag{6}$$

which is to be solved for $V(x)$ as a function of x, with the boundary condition

$$V(x) = V_0 \text{ at } x = 0. \tag{7}$$

Here, V_0 is the velocity at the position of maximum jet swell, which is taken as the origin of our coordinate system. V_0 is determined from eq. (2) since the filament diameter at the position of maximum jet swell is photographically measured. However, in solving eq. (6) one has to know $C(x)$, the concentration profile of solvent, in the elongating filament along the spinning way. This necessitates solving a mass balance equation together with eq. (6). As noted above, a thorough investigation of the mass transfer process in wet spinning is a complicated matter. Therefore, the authors follow a less rigorous approach and take the mass transfer into account by

$$W\frac{dC(x)}{dx} = -k_m 2\pi R(x)[C(x) - C_b] \tag{8}$$

where W is the mass flow rate of dope, $C(x)$ is the weight fraction of solvent in the fiber (on a polymer-free basis), k_m is an overall mass transfer coefficient (g/sec cm^2), $R(x)$ is the radius of the elongating filament, and C_b is the bath concentration of solvent. The assumptions made in formulating eq. (8) are: (1) a flat concentration profile within the filament at any position x; (2) a constant bath concentration, which is the equilibrium concentration of solvent in the filament.

Equation (8) may be rewritten by replacing $R(x)$ with $V(x)$ from eq. (2):

$$\frac{dC(x)}{dx} = \frac{-2k_m}{\rho}\sqrt{\frac{\pi}{Q}}\frac{C(x) - C_b}{\sqrt{V(x)}} \tag{9}$$

where ρ is the density of filament. Equation (9) is to be solved for $C(x)$ with the boundary condition

$$C(x) = C_0 \text{ at } x = 0 \tag{10}$$

where C_0 is the concentration of solvent in the dope on a polymer-free basis.

We thus have two nonlinear differential equations, (6) and (9), two boundary conditions, (7) and (10), and three empirical constants, A, B, and k_m. These two equations are integrated numerically to yield both velocity and concentration profiles along the spinning bath. Since A, B, and k_m are not known a priori, these numerical integrations are repeated for several combinations of these constants to determine parameter sensitivity. Since the experimentally measured velocity and elongational viscosity profiles are known for a given set of spinning conditions, the constants A, B, and k_m

are adjusted until the theoretically calculated profiles coincide satisfactorily with the experimentally obtained profiles. At this point, it may be assumed that the concentration profile is reasonably acceptable. This approach, though crude, will give some insight into the coagulation phenomenon, especially if the system is not overly sensitive to variations in A, B, and k_m.

EXPERIMENTAL

The spinning apparatus and spinning solution have been described in detail in part I of this series.[9] The spinning dope was an aqueous solution of polyacrylonitrile (PAN) in sodium thiocyanate (NaSCN). The coagulating bath solution was NaSCN in water, varying in concentration from 0% through 25% (weight per cent). Temperature was varied from 0°C to 40°C.

Filament tension was measured with a tensiometer at various positions of the take-up roll, as described in part I. Filament diameter and free diameter were measured by photographing the individual filament as a function of position x. For a constant density filament, diameter $D(x)$ and velocity $V(x)$ are related by

$$Q = \frac{\pi}{4} D^2(x) V(x) \tag{11}$$

or

$$V(x) = \frac{4Q}{\pi D^2(x)} \tag{12}$$

where Q is the volumetric flow rate through the spinnerette. Thus, the velocity profile is also obtained from the photographic measurement of filament diameter.

Circular-die spinnerettes of diameter 0.005, 0.012, and 0.015 in. were used. The apparent shear rate, $\dot{\gamma}$, in all capillaries was kept constant at 1.02×10^4 sec^{-1} in most experiments (except where indicated). Since the shear rate is given by

$$\dot{\gamma} = \frac{4Q}{\pi R^3} = \frac{8V_1}{D_1}, \tag{13}$$

the volumetric throughput Q (or the average velocity in the spinnerette, V_1) was varied as the spinnerette hole diameter D_1 was varied in order to keep $\dot{\gamma}$ constant.

The following parameters of the spinning process, which will be defined below, were measured or calculated: the average velocity through the spinnerette hole V_1; the take-up velocity V_2; the free velocity V_f; and the free diameter D_f; the free jet stretch (the ratio of take-up velocity to free velocity) V_2/V_f; the maximum take-up velocity before filament breakage

V_{2m}; the total tension per filament at the take-up rolls F_{tot}; the filament diameter as a function of distance from the spinnerette face $D(x)$.

RESULTS AND DISCUSSION

The Free Jet Velocity and Free Jet Diameter of Wet-Spun Filaments

A measure of the spinnability of a given material under continuous spinning conditions has been defined as the jet stretch V_2/V_1,[3,6,9] with V_2 being the velocity of the filament at the take-up roll and V_1 the plug flow spinnerette velocity. The magnitude of this quantity is often less than 1, although high fiber attenuation is nevertheless attained. However, if instead of V_1 one uses the free velocity V_f, which is defined as the velocity of a freely extruded stream, the jet stretch V_2/V_f becomes greater than unity under usual spinning conditions. This is because the free velocity is much smaller than the velocity in the spinnerette, as can be shown from the mass balance equation

$$V_f = V_1(D_1/D_f)^2 \tag{14}$$

in which D_1 is the spinnerette hole diameter and D_f is the maximum attainable (free) fiber diameter. It is to be noted that D_f is greater than D_1 for viscoelastic fluids, a fact that is attributed to the release of elastic energy stored by the viscoelastic fluid at the die exit. In effect, D_f is the true

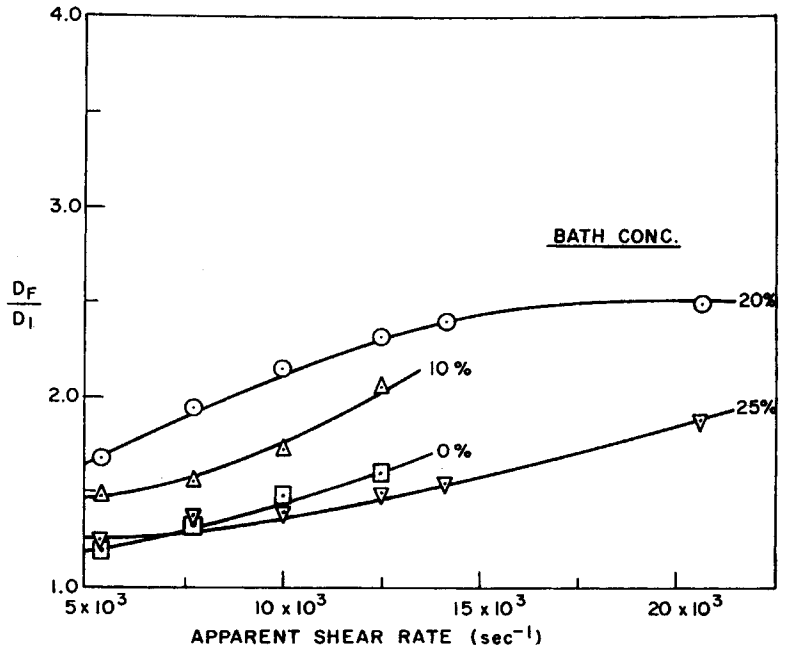

Fig. 1. Jet swell vs. apparent shear rate in spinnerette holes. Spinnerette diam. = 0.005 in.; bath temp. = 20°C.

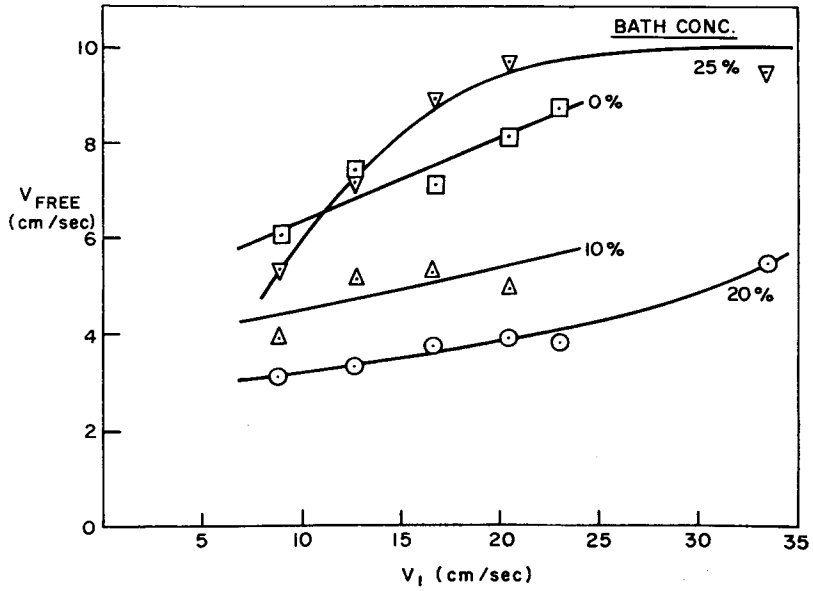

Fig. 2. Free jet velocity vs. throughput velocity. Spinnerette diam. = 0.005 in.; bath temp. = 20°C.

initial diameter and V_f is the true initial velocity, which is the basis for measuring true filament attenuation. It should be noted that D_f is dependent on spinnerette hole design, shear rate, rheological properties of the dope, temperature, and coagulating bath conditions. Thus, a more realistic measure of spinnability and of filament attenuation is the "free jet stretch," V_2/V_f. In the presentation of the results, we shall use the jet stretch based on the free jet velocity V_f, unless otherwise noted.

Curves of D_f/D_1 versus apparent shear rate $\dot{\gamma}$ and of the free velocity V_f versus throughput velocity V_1 are presented in Figures 1 and 2, respectively, for various bath concentrations and for spinnerette diameter D_1 equal to 0.005 in. The free jet swell ratio D_f/D_1 increases with bath concentration, except for the anomalous 25% concentration curve, which will be discussed below. The free jet swell ratio also increases with shear rate (or throughput), a result also presented by Paul[3] for a different wet-spinning system. Between 0% and 20% bath concentration, the increase in jet swell ratio with bath concentration is believed to be due to the decrease in coagulation rate (hardening). This speculation is based on the fact that wet-spun fiber formation involves formation of a solid, coagulated skin which acts as a barrier to further coagulation.[3,4,7] Once the skin is formed, it limits the degree of swelling. The formation of skin would be faster as the driving force for the mass transfer between the extruded filament and coagulating bath is greater, and hence as the bath concentration is lower. The increase in D_f/D_1 with throughput velocity V_1 can be attributed to the higher degree of recoverable shear at the tube exit.

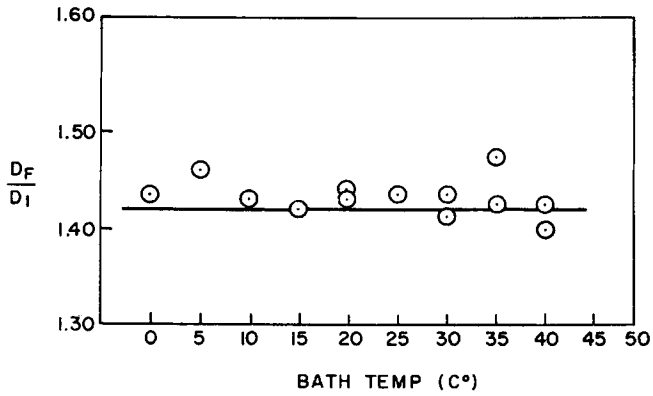

Fig. 3. Jet swell vs. bath temperature. Spinnerette diam. = 0.005 in.; bath concn = 10%; shear rate = 10^4 sec^{-1}.

It should be noted here that the results in Figures 1 and 2 are similar to the results presented by Paul,[3] but with some differences. The differences are due to the fact that different polymer–coagulant systems are under consideration, because the degree of swelling is extremely dependent upon the system under consideration.

Free jet diameter D_f as a function of temperature was also measured, and in Figure 3 it is seen that free jet diameter is practically independent of the bath temperature. This phenomenon was also noted by Paul.[3] In all probability, temperature does have some effect on the free jet diameter, but this effect is small relative to the more pronounced concentration effects.

As can be seen from Figures 1 and 2, and as is discussed in part I,[9] the diameter of a freely extruded filament is smaller at a bath concentration of 25% NaSCN than at 20%. It has been postulated that at such high bath concentrations and low rates of coagulation, skin formation is effectively retarded, and the entire extruded filament swells into a gel-like structure. The coagulant then does not effectively extract the solvent from the filament, but rather partially dissolves the polymer.[7] Swelling of gels is limited, as is dissolution of such gels, by the unfavorable polymer–solvent interaction. Thus, this particular behavior cannot be generalized to all polymer–solvent systems, and this would then explain the surprisingly lower values of D_f/D_1 for 25% NaSCN in Figure 1. Since the free jet swell ratio, D_f/D_1, is a measure of the degree of coagulation, minimum "hardening" is assumed to occur at the maximum of D_f/D_1. For our system, therefore, actual hardening is effectively minimized at 20% bath concentration, rather than at higher concentrations, independent of spinnerette hole size.

The Effect of Coagulating Bath Conditions on Maximum Jet Stretch

It is clear that for a given throughput rate, the take-up velocity cannot be increased indefinitely. At a maximum take-up velocity, V_{2m}, the fila-

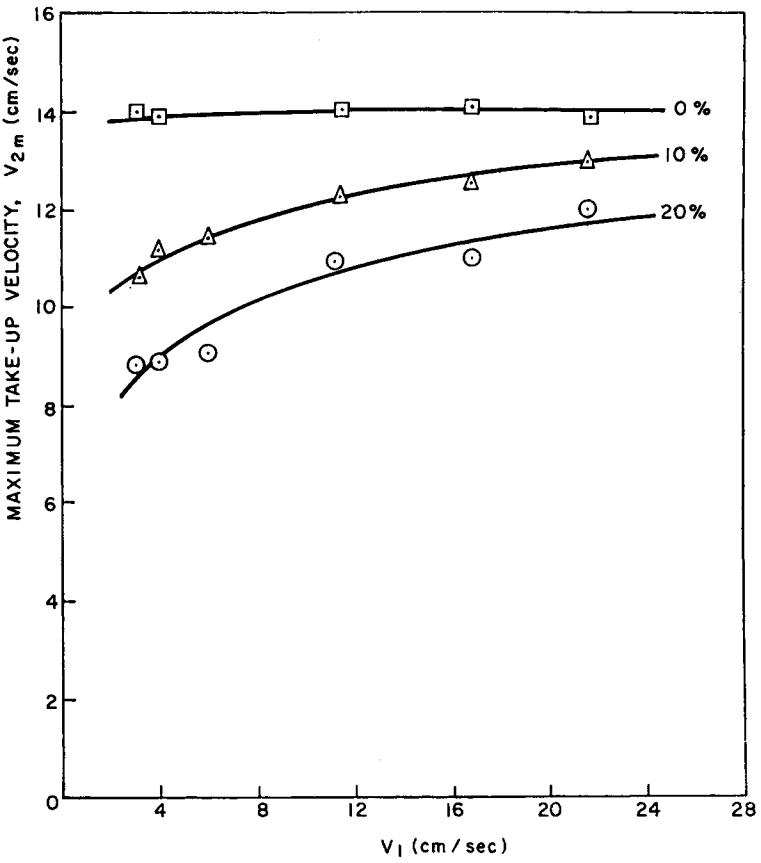

Fig. 4. Maximum take-up velocity vs. throughput velocity. Spinnerette diam. = 0.005 in.; bath temp. = 20°C; shear rate = 10^4 sec^{-1}.

ments begin to break in the bath at or near the face of the spinnerette. Spinning at this maximum velocity is just stable, since the continuous drawing of filaments cannot be realized above this critical value of take-up velocity. This maximum take-up velocity is a quantity depending on the spinning variables, such as the properties of spinning dope, composition and temperature of the coagulating bath, throughput rate, etc.

Figure 4 shows plots of V_{2m} versus V_1 at various values of bath concentration. It is seen that below 20% bath concentration, the maximum take-up velocity decreases as the bath concentration increases. The maximum V_{2m} is attained at the condition of maximum coagulation rate, i.e., 0% bath concentration. In addition, the maximum take-up velocity V_{2m} is seen to increase as the throughput velocity increases. A similar result is reported by Paul.[3] Both of these results are in agreement with general expectations.

Figure 5 shows the plots of maximum jet stretch $(V_2/V_f)_m$ versus bath concentration at various values of throughput rate. Again, as expected,

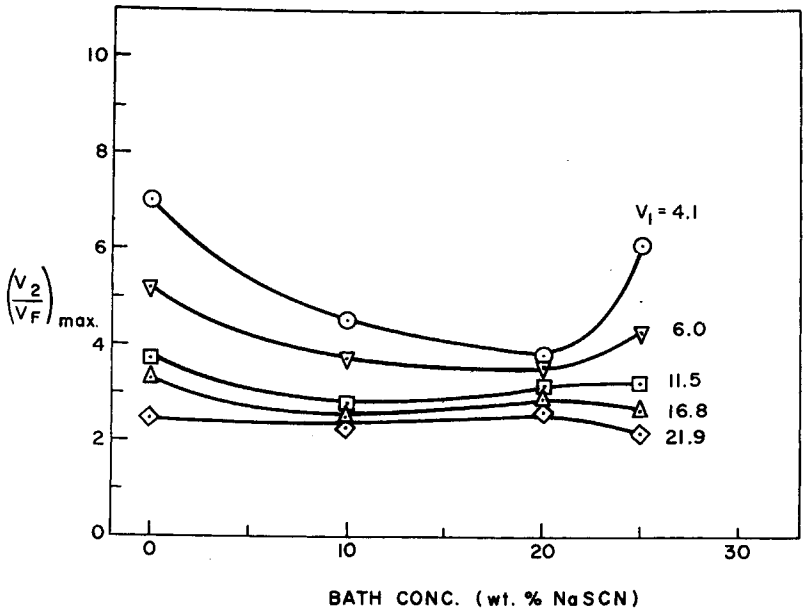

Fig. 5. Maximum jet stretch vs. bath concentration. Spinnerette diam. = 0.005 in.; bath temp. = 20°C; shear rate = 10^4 sec^{-1}.

the maximum jet stretch decreases as bath concentration increases up to 20% NaSCN. It is to be noted, however, that the 25% NaSCN bath concentration does exhibit anomalous behavior, which may be explainable by the discussion given previously. Since the free diameter D_f at 25% is small, the free velocity V_f is correspondingly high, see eq. (14). The high free jet velocity gives a high take-up velocity before thread breakage, although at this high bath concentration the thread is a wet, gelatinous filament, confirming our deduction regarding the hardening mechanism. As would also be expected, decreasing the bath temperature increases V_{2m} and $(V_2/V_f)_m$. This is probably caused by the strong viscosity dependence on temperature, as will be discussed below.

The Distribution of Tensile Stress Along the Spinning Way

As was discussed above in connection with the force balance equation for the wet-spinning system, the total tensile stress needed to draw and elongate a filament increases as the distance between the take-up roll and spinnerette increases. The internal tensile force, F_{rheo}, however, is of constant magnitude over the distance in which deformation occurs. The procedure for determining F_{rheo} from the experimental measurement of F_{tot} is given in part I of this series.[9] Since the cross-sectional area of any elongating filament decreases with distance, the tensile stress p_{xx}, defined by eq. (1), of course increases with distance and approaches a limiting value as the rate of deformation decreases. Figure 6 shows the plots of tensile

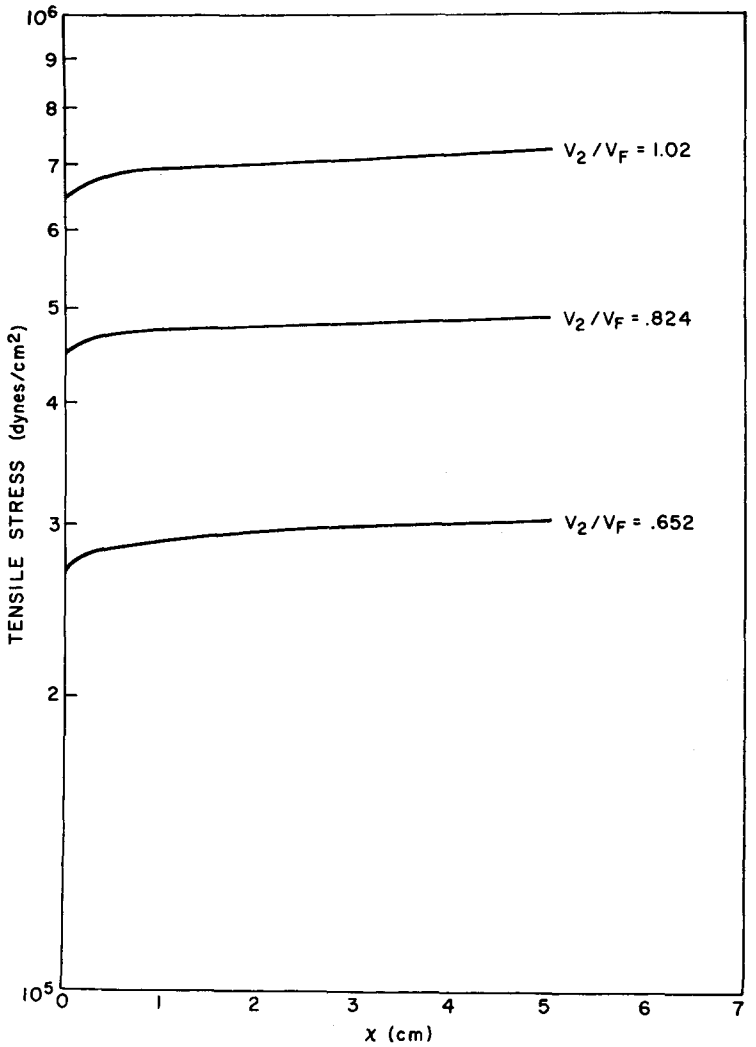

Fig. 6. Tensile stress vs. spinning distance. Spinnerette diam. = 0.005 in.; bath temp. = 20°C; bath concn. = 10% NaSCN.

stress versus distance x for a few values of jet stretch. The curves have very low slopes, except near the spinnerette face where the filament undergoes its greatest deformation.

It is of interest to note the effect of throughput and take-up velocity on (total) tension at a given value of take-up distance. Figure 7 presents total take-up tension at $x = 60$ cm as a function of free jet stretch V_2/V_f, with the throughput velocity V_1 as a parameter. It is seen that as the throughput increases, the tension curves become a steeper function of the take-up rate. It is also interesting to note that the maximum take-up velocity V_{2m} increases as the throughput rate increases.

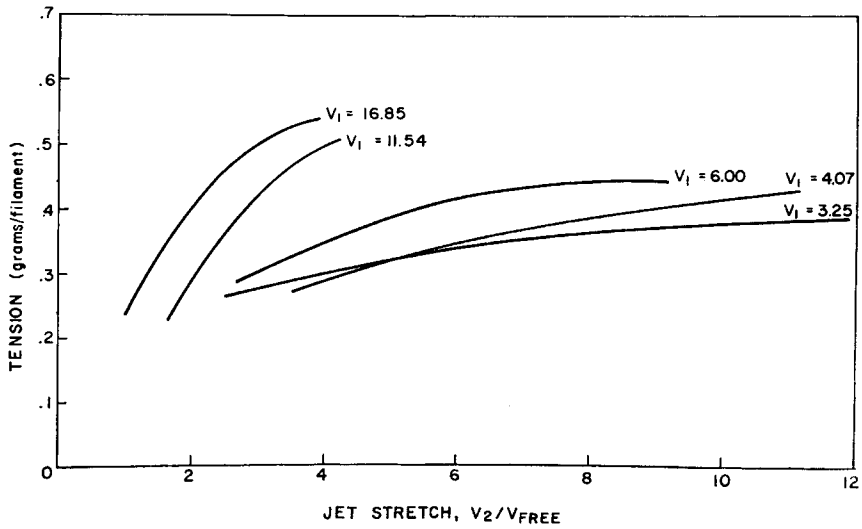

Fig. 7. Total tension vs. jet stretch. Spinnerette diam. = 0.005 in.; bath temp. = 20°C; bath concn. = 10% NaSCN.

The Effect of Coagulating Bath Conditions on Tension

Figure 8 shows the effect of the bath concentration on the total measured tension at the take-up device (x = 60 cm) for a representative value of V_2/V_1. Here, V_2/V_1 rather than V_2/V_f is used since V_f is itself a function of

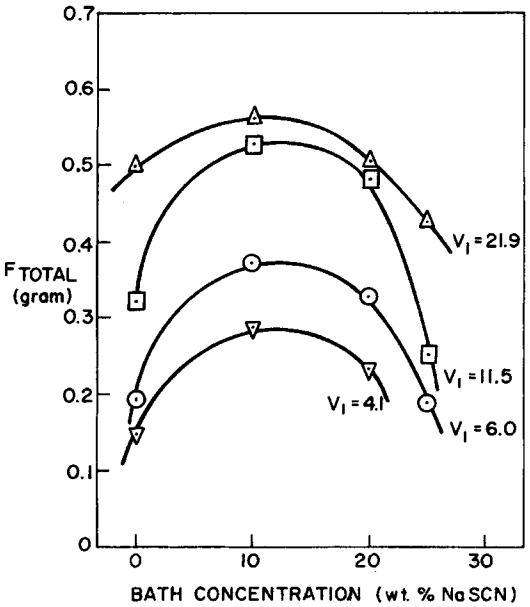

Fig. 8. Total tension vs. bath concentration. V_2/V_1 = 1.0; x = 65 cm; bath temp. = 20°C.

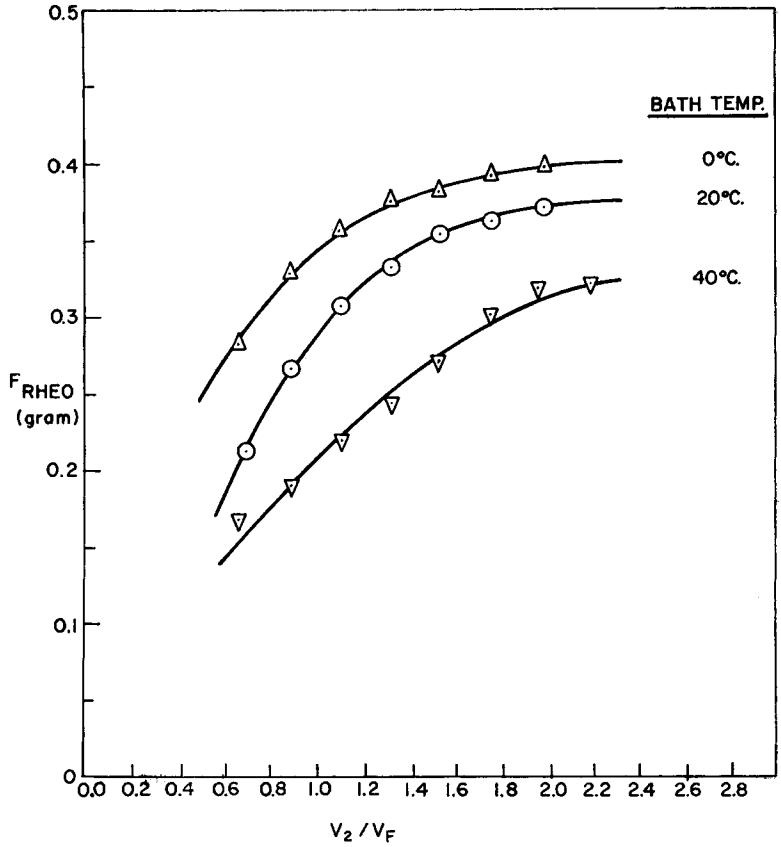

Fig. 9. F'_{rheo} vs. jet stretch. V_1 = 16.62 cm/sec; bath concn. = 10%; spinnerette diam. = 0.005 in.

bath concentration. It is seen that all the curves behave in a similar manner. Note that the tensile force goes through a maximum for a bath concentration of about 10% NaSCN. This is extremely significant since it is known that commercial spinning is usually carried out with a comparable concentration of solvent in the coagulating bath (for this system). Undoubtedly the higher tension at this bath concentration increases spinnability and/or minimizes the possibility of thread breakage. Spinning under maximum tension, and therefore under maximum tensile stress, may also improve the tensile properties of the finished fiber by increasing molecular orientation in the preliminary (i.e., prewash) stages of the spinning process.

There are thus two apparent criteria for determining fiber spinnability. While filament tensions have a maximum at a bath concentration of 10%, the take-up velocity has a maximum at 0% NaSCN (and at the commercially undesirable 25% value described above). This will be discussed at length below.

Figure 9 shows F_{rheo} versus jet stretch V_2/V_f as a function of temperature. A similar relationship exists for F_{tot}. It is seen that the take-up force, and therefore tensile stress, increases as the temperature decreases. It is interesting to note, however, that coagulation rate decreases as the temperature decreases, while the tension increases as temperature decreases.

The Distribution of Elongational Viscosity Along the Spinning Way

The dependence of elongational viscosity η_E on elongation rate dV/dx and jet stretch has been discussed at length by the authors in part I of this paper.[9] From Figure 10 it is seen that η_E increases with distance x for all spinnerette hole diameters. Physically, such behavior is caused by coagulation of the fluid filament. As coagulation proceeds, the rate of change of filament diameter decreases. As this rate of deformation decreases, it is seen from the definition of elongational viscosity, eq. (1), that η_E increases and eventually approaches infinity. However, infinite η_E is never physically realizable since F_{rheo} is not defined at the point where deformation ceases.

In Figure 10 it is seen that η_E is a function also of spinnerette diameter. This geometry dependence sounds strange when determining such fundamental rheological properties as elongational viscosity. However, such geometry dependence is accounted for by the fact that hardening is occurring and that it greatly influences the magnitude of the elongational viscosity. To minimize hardening, it is necessary to limit heat and mass transfer. This is accomplished by spinning under isothermal conditions and at high bath concentrations. As explained above, minimum hardening, as measured by free jet swell, occurs at approximately 20% bath concentration for our system.

A third method of decreasing the effects of coagulation is to decrease the percentage of coagulated skin per unit volume of filament. Experimentally, this amounts to increasing the spinnerette diameter. Since the depth of coagulated skin is a function of time,[3,4] a fiber of larger diameter will retain a larger volume percentage of fluid "core" over a given period of time. As shown in Figure 10, the magnitude of η_E actually does decrease as the spinnerette diameter increases. A detailed description of the dependence of elongational viscosity on bath concentration, temperature, and spinnerette diameter is given in part I of this series.[9]

The increase in η_E along the spinning way, which for wet spinning is attributed to the coagulation in the bath, is very similar to that found in melt spinning by Ziabicki,[11] who showed an increasing trend of η_E along the spinning way. In the case of melt spinning, the increase in η_E along the spinning way is attributed to the cooling effect. Therefore, one can see that elongational viscosity increases with the spinning distance due to coagulation in wet spinning and cooling in melt spinning, regardless of the magnitude of the elongation rate. Therefore, in actual spinning processes,

the effect of elongation rate on elongational viscosity is negligibly small compared to the effect of the hardening process. It should be noted here that hardening is concurrently accompanied by a decrease in the magnitude of the rate of elongation. It may further be surmised that the increase in

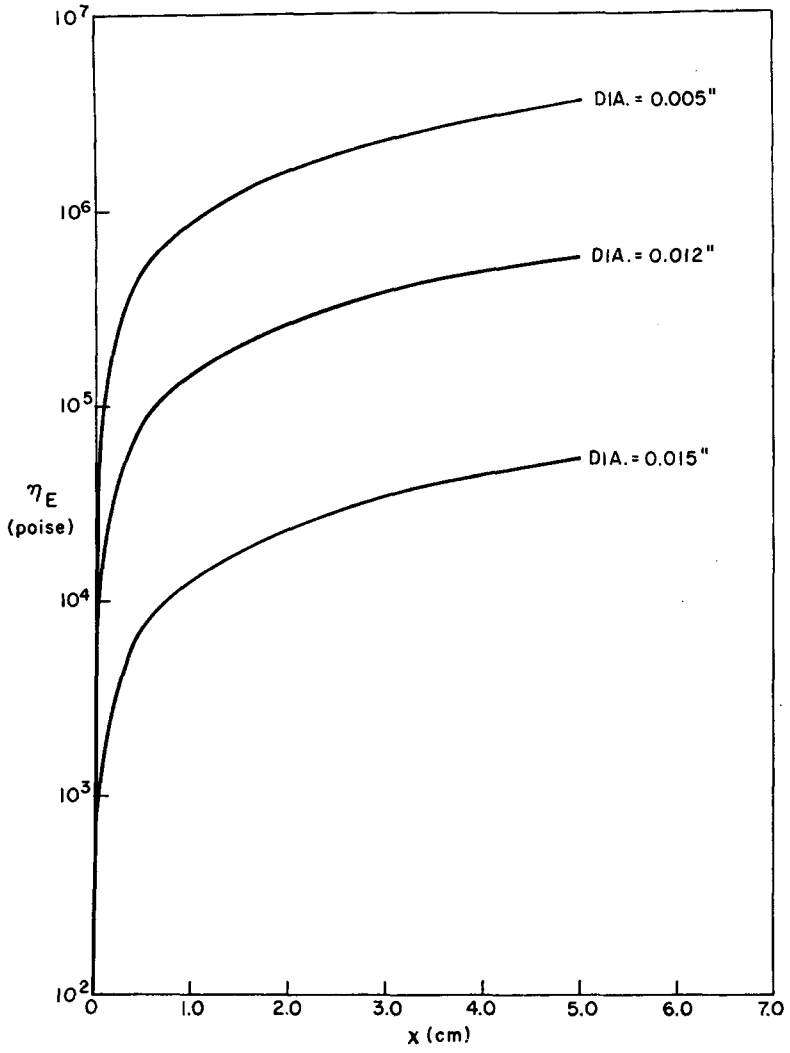

Fig. 10. Elongational viscosity vs. spinning distance. $V_2/V_f = 2.6$; bath concn. = 20% NaSCN; bath temp. = 20°C.

elongational viscosity along the spinning way is a necessary condition for spinnability. Also note that the distribution of elongational viscosity along the spinning way strongly influences the physical properties of the finished product.

Spinnability and the Breakage Mechanism

Three factors which could affect spinnability and the mechanism of fiber breakage in the wet-spinning process may be isolated from the above discussion: (1) bath concentration; (2) system temperature; and (3) jet stretch. Bath concentration is important because this factor actually determines the rate of coagulation, skin formation, free velocity and maximum jet stretch, and tensile stress. Temperature is important primarily because it affects the structural viscosity of the spinning solution: the main effect of temperature is thus upon tensile stress and jet stretch rather than upon coagulation rate. Jet stretch is listed independently because it is actually a measure of the filament residence time in the bath; the larger the jet stretch, the shorter the filament residence time. Even under optimum conditions of temperature and concentration, the jet stretch may be considered to be an independent variable.

It has been stated that commercial spinning is performed under conditions of moderate bath concentration and at low temperatures. These conditions are probably close to optimum since solution viscosity, jet stretch, and coagulation rate are balanced so as to allow near-maximum tensions, near-maximum jet stretch, and probably the minimum chance of thread breakage.

At extremely low bath concentration, which brings rapid coagulation, the maximum tension attainable and the maximum jet stretch are both limited. This limitation may be caused by the breakage of the filament "skin," since at a very low bath concentration the rapid hardening causes formation of a solid skin which inhibits further coagulation of the fluid core.[3-5] The resultant breakage can be caused by "slippage" between the solid annular skin and the fluid core. Thus, this mechanism may be more dependent on maximum take-up velocity V_{2m} than on tensile stress.

At somewhat higher bath concentrations, slower skin formation allows more thorough hardening of the entire fiber, and an optimum filament strength dependent on coagulation rate may be achievable. Breakage of the "slowly hardened" filament would then occur if a critical tensile stress is exceeded, and at this point the hardened portion would separate completely from the fluid (at or in the spinnerette) over the entire cross section of the filament. This mechanism is slightly different from the one proposed by Paul,[3] since in his proposed "second" mechanism the skin is ruptured because of an excessive tensile stress, and this leads to filament breakage because the fluid core could not support the tension. In effect, Paul assumes a two-phase filament independent of coagulation rate, while the mechanism proposed here suggests that if coagulation is slow enough, the filament is effectively hardened throughout. This second mechanism would also apply in the case of the "gel" structure resulting from very high bath concentrations (e.g., over 25%). Realistically, all three proposed mechanisms are probably partially true and contribute to the true fiber breakage phenomenon.

It follows, therefore, that there is an optimum coagulation rate which is a function of bath temperature and concentration and which maximizes the combination of fluid and skin strength of the partially hardened fiber. Temperature may play a dual role here, since the effect of temperature on the dope viscosity appears to be more important than its effect on coagulation rate.

The two mechanisms proposed here and the two proposed by Paul[3] are completely different from those hypothesized by Ziabicki[2] in his early study of thread breakage. Ziabicki investigated the breakage of fluids of varying degrees of viscoelasticity and also presented two breakage mechanisms. The "cohesive" break, according to Ziabicki, is a "result of tensile stress at high rates of deformation" and occurs only in elastic liquids since purely viscous liquids dissipate all energy of deformation instantly. The "capillary" break occurs at low flow rates in ideally viscous liquids. The cohesive break of a thread resembles the break of a brittle solid, while the capillary break occurs simultaneously at several points along a liquid (e.g., water) thread. The breakage of any real fluid thread is, of course, a composite of these two ideal cases.

Concentration Profile of Solvent in the Fiber

The approximate concentration profile of solvent, NaSCN, in the fiber was obtained by solving the mass balance equation, eq. (9), simultaneously with the force balance equation, eq. (6), the boundary conditions being given by eqs. (10) and (7). These two differential equations were solved numerically by a fourth-order Runge-Kutta predictor-corrector method,

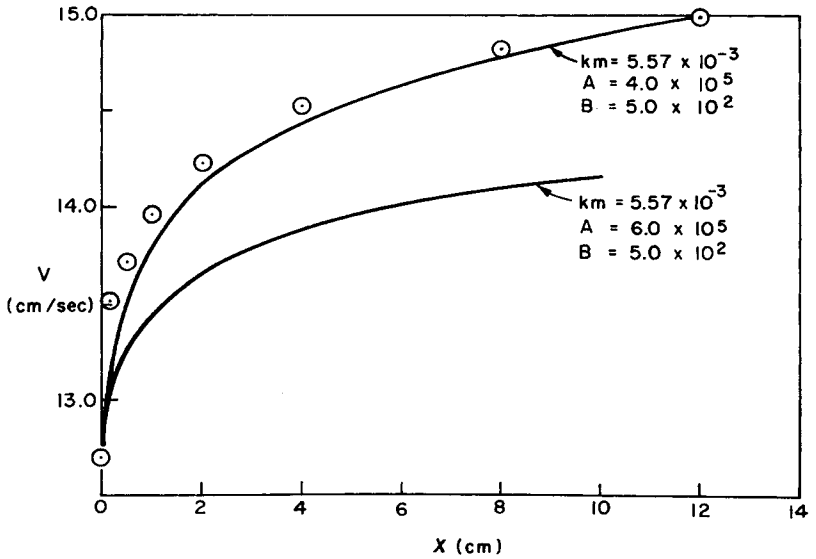

Fig. 11. Filament velocity vs. spinning distance. V_2/V_f = 1.96; spinnerette diam. = 0.015 in.; bath temp. = 20°C; bath concn. = 20% NaSCN.

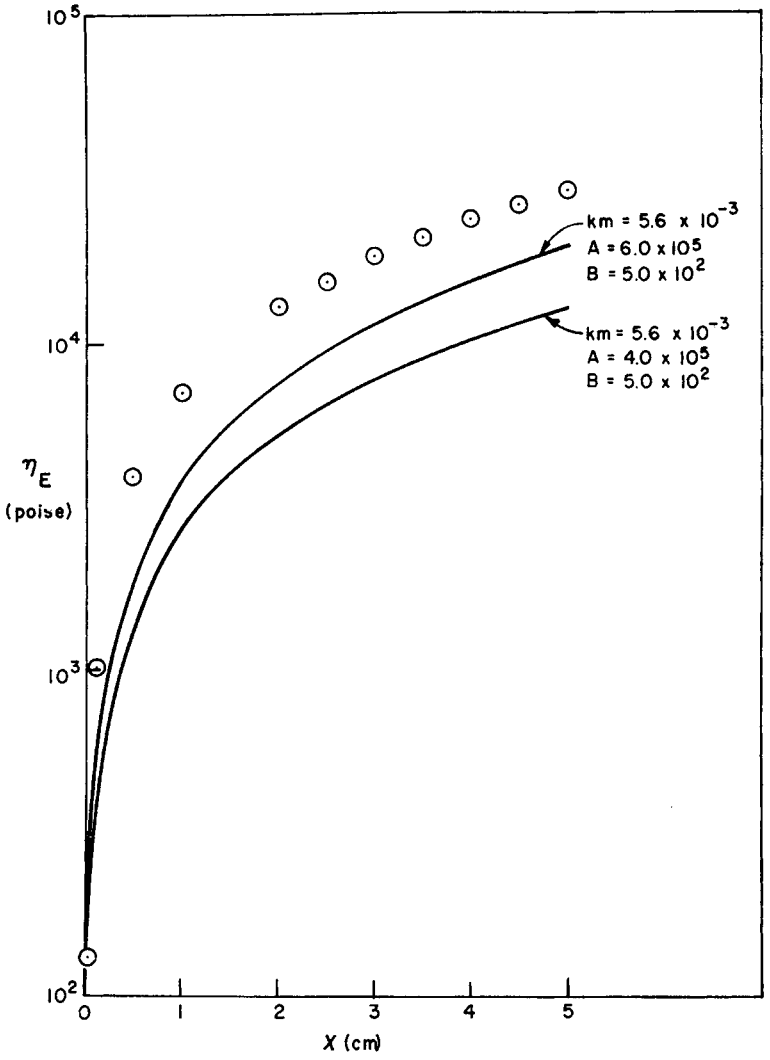

Fig. 12. Elongational viscosity vs. spinning distance. V_2/V_f = 1.96; spinnerette diam. = 0.015 in.; bath temp. = 20°C; bath concn. = 20% NaSCN.

and the values of the empirical constants k_m, A, and B had to be supplied.

The experiment simulated was one of very slow coagulation rate: bath concentration, 20% NaSCN; bath temperature, 20°C; spinnerette diameter, 0.015 in.; and $V_2/V_f = 1.95$. The initial velocity V_0 was 12.7 cm/sec, and the initial concentration C_0 was 0.484 g NaSCN/g spinning solution (polymer free). The empirical constants were varied until the experimentally determined velocity and viscosity data were matched by the curves predicted by eqs. (6) and (4), respectively. At this point, it was assumed that the concentration profile was determined.

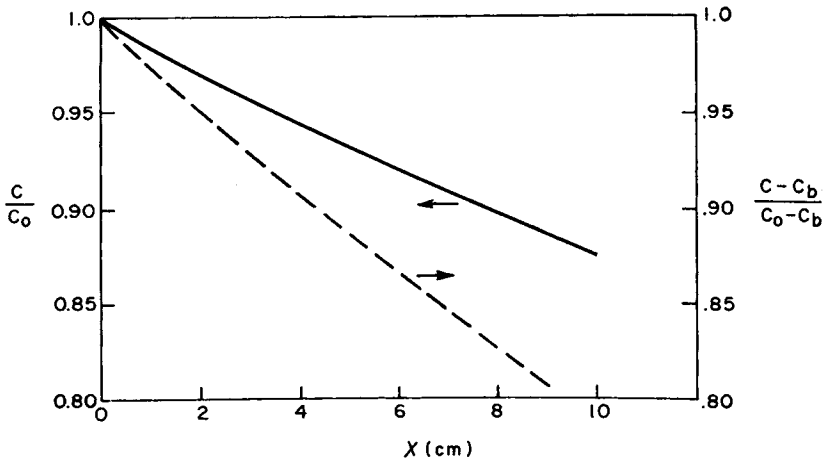

Fig. 13. Concentration profile of solvent in the fiber. $V_2/V_f = 1.96$; spinnerette diam. = 0.015 in.; bath temp. = 20°C; bath concn. = 20% NaSCN; $C_0 = 0.484$; $C_f = 0.20$.

The best value of k_m as determined by the above procedure was 0.00557 g/cm sec^2, or 6.85×10^{-5} g-mole/cm sec^2, a realistic order of magnitude for this constant. Figure 11 shows plots of both the experimental and theoretical velocity profile for two sets of empirical constants, A and B. From eq. (9) it is seen that the concentration of solvent in the filament, $C(x)$, is dependent upon the square root of the filament velocity $V(x)$. Since $V(x)$ does not vary appreciably along the spinning way, $C(x)$ is not strongly dependent upon $V(x)$, or therefore upon parameters A and B. Thus, the given value of k_m is the best value for both sets of constants A and B given in Figure 11.

Figure 12 shows plots of both experimentally and theoretically determined elongational viscosity as a function of x. The best value of the parameter A determined was approximately 10^6, and the best value of B determined was approximately -10^3. For a maximum value of $C_0 - C(x)$, which is about 0.20, the second term on the right hand side of eq. (5) is three orders of magnitude larger than the third term, indicating that the elongational viscosity is (approximately) linearly dependent upon the solvent concentration in the filament. From Figures 11 and 12, it is seen that as A increases, the calculated elongational viscosity curves approach the experimental data, but the calculated velocity curves depart from the experimental data. The experimentally determined velocity profile, however, is considered to be more accurate than the experimentally determined elongational viscosity. That is because the velocity profile is directly measured, while the elongational viscosity is calculated from the measurements of other variables. Thus, the best values of A and B determined were 4.0×10^5 and -10^3, respectively, and with these values of A and B, a reasonably good fit to the velocity data was obtained.

Figure 13 shows the resultant concentration profile of solvent in the fiber. It must be borne in mind that this model is only a physical approximation and is most accurate over a short distance near the spinnerette, where appreciable thread deformation occurs. From Figure 13 it is seen that approximately 94% of the original concentration of solvent remains in the filament at the distance of 4 cm from the spinnerette face. Since $C(x)$ can never go below the equilibrium (bath) concentration C_b, a measure of solvent removal with respect to the maximum amount of solvent which can be removed is $[C(x) - C_b]/(C_0 - C_b)$. This quantity is also plotted in Figure 13, and it is seen that when 6% of the original solvent is removed from the fiber, the solvent concentration has moved toward equilibrium by approximately 10%. By either measure, the percentage of solvent removed from the filament is very low. This is actually not surprising, since the concentration difference between the filament and the bath is very low. Furthermore, we are considering the average concentration in the filament at any position x.

At the surface of the filament, the concentration of solvent is, of course, very low, but this skin only accounts for a fraction of the total filament volume. It is clear from Figure 13 that most of the solvent must be removed from the filament in subsequent operations (washing), rather than during the coagulation and drawing step.

Lastly, it should be noted that the mass transfer mechanism postulated in the present study does not hold true beyond a certain distance away from the spinnerette face, where the diffusion of solvent through a hard "skin" of the filament is a controlling mechanism. It should also be noted that essentially all of the thread deformation (i.e., elongation) occurs in a relatively short distance from the spinnerette face. Therefore, one can surmise that when there is no deformation in the spinning way, the force balance equation, eq. (6), loses its meaning, as does the mass balance equation, eq. (9). Some authors[12] have made a study of mass transfer due to the diffusion mechanism for a spinning system similar to the one reported in this paper.

CONCLUSIONS

Polyacrylonitrile in an aqueous solution of sodium thiocyanate is wet spun under commercial spinning conditions. The following conclusions may be drawn from the present study.

1. A suggestion is made that the jet stretch V_2/V_f, based on free jet diameter, be used as a true measure of filament attenuation. Here, V_2 is the take-up velocity and V_f is the free jet velocity.
2. The free jet swell ratio D_f/D_1 increases as the throughput rate (and hence shear rate) increases.
3. The free jet swell ratio increases as the bath concentration increases from 0% NaSCN to 20% NaSCN, but decreases as the bath concentration

exceeds 20% NaSCN. If the free jet swell is used as a measure of hardening, then hardening may be assumed minimal at 20% bath concentration.

4. Below 20% bath concentration, it is found that the maximum take-up velocity V_{2m} decreases as the bath concentration increases (i.e., as the rate of coagulation decreases).

5. The measured tensile force is a maximum at a bath concentration of roughly 10% NaSCN. This is approximately the bath concentration used commercially.

6. Elongational viscosity η_E increases with distance from the spinnerette face. The magnitude of η_E is dependent on bath concentration.

7. At high rates of coagulation, rapid skin formation is encountered, and fiber breakage is assumed to occur because of "slippage" between the solid skin and fluid core. At low rates of coagulation, the fiber is more uniformly coagulated, and fiber breakage occurs because of a more uniform separation between coagulated and uncoagulated jet.

8. Based on the model presented here, only a small percentage of solvent is removed from the interior of the filament during the coagulation step. This indicates that the washing and treatment steps are of major importance in solvent removal, while the particular bath concentration is most important in the determination of the spinning conditions.

The work was supported in part by a grant from Solvay et Cie., for which the authors are grateful. The authors are also grateful to Drs. D. J. Johnson and S. N. Chinai of the American Cyanamid Company, who kindly supplied the authors with a large quantity of the materials for the spinning experiments.

This work is taken in part from the dissertation of L. Segal, submitted to the Faculty of the Polytechnic Institute of Brooklyn in partial fulfillment of the requirements for the degree of Doctor of Philosophy, 1970.

References

1. A. Ziabicki, *Kolloid-Z. Z. Polym.*, **175**, 14 (1961).
2. A. Ziabicki, *Bull. Acad. Polon. Sci. Ser. Tech.*, **12**, 1 (717); 9 (725); 21 (821) (1964).
3. D. R. Paul, *J. Appl. Polym. Sci.*, **12**, 2273 (1968).
4. D. R. Paul, *J. Appl. Polym. Sci.*, **12**, 383 (1968).
5. H. F. Mark, in *Rheology*, Vol. 4, F. R. Eirich, Ed., Academic Press, New York, 1964.
6. W. E. Fitzgerald and J. P. Craig, *ACS Preprints*, New York, 1966.
7. E. Cernia, in *Man Made Fibers*, Vol. 3, H. Mark, S. Atlas, and E. Cernia, Eds. Wiley, New York, 1967.
8. C. D. Han, *Rheol. Acta*, **9**, 355 (1970).
9. C. D. Han and L. Segal, *J. Appl. Polym. Sci.*, **14**, 2973 (1970).
10. F. T. Trouton, *Proc. Roy. Soc. L*, **77**, 426 (1906).
11. A. Ziabicki and R. Takserman-Krozer, *Kolloid-Z. Z. Polym.*, **199**, 9 (1964).
12. H. Takeda and A. Kato, *Kogyo Tagaku Zasshi*, **67**, 1285 (1964).

Received May 4, 1970